

Using Remote Sensing to Map and Monitor Water Resources in Arid and Semiarid Regions

Victor Klemas and Aline Pieterse

Contents

1	Introduction	34
2	Identification and Mapping of Arid and Semiarid Regions	35
3	Detecting and Mapping Inland Surface Waters	36
4	Detecting Subsurface Waters	38
4.1	Determining Soil Moisture	38
4.2	Detecting Groundwater	41
5	Detecting Freshwater Springs and Biomass	44
5.1	Detecting Freshwater Plumes	45
5.2	Determining Biomass Production	46
5.3	Biomass as a Drought Indicator	47
6	Detecting and Mapping Wetlands	48
7	Drought Monitoring and Prediction	51
8	Conclusions	52
	References	54

Abstract Life on Earth depends on water. Yet water resources are severely stressed by the rapid growth of the human population and activities. In arid environments the exploration and monitoring of water resources is a prerequisite for water accessibility and rational use and management. To survey large arid areas for water, conventional land-based techniques must be complemented by using satellite and airborne remote sensors. Surface water systems can be mapped using multispectral and radar sensors; soil moisture in the unsaturated zone can be remotely sensed with microwave radiometers using indirect indicators, such as

V. Klemas (✉)

School of Marine Science and Policy, University of Delaware, Newark, DE, USA

e-mail: klemas@udel.edu

A. Pieterse

Department of Geological Sciences, University of Delaware, Newark, DE, USA

microwave emissivity; freshwater wetlands can be mapped using multispectral cameras; and freshwater springs can be detected using thermal infrared radiometers. Satellite remote sensors and satellite gravitational surveys can be used in combination with ancillary data analysis to infer groundwater behavior from surface expressions and to estimate groundwater aquifer storage. This chapter provides an overview of satellite and airborne remote sensing techniques for managing water resources and monitoring drought in arid and semiarid regions.

Keywords Groundwater exploration • Remote sensing springs • Soil moisture sensing • Water remote sensing • Wetland mapping

1 Introduction

Only a small fraction of the Earth's water is available as freshwater, a key resource in many economic activities ranging from agriculture to industrial production. At present, water resources are severely stressed and particularly scarce in arid regions of the world. In many arid and semiarid regions, water shortage is a major obstacle to sustainable development and poverty alleviation and the cause of serious conflicts between some countries. Water shortage in arid regions can be further aggravated by the global climate change that is predicted to severely impact these regions. Thus, exploration, mapping, and monitoring of water resources are a prerequisite for the availability, accessibility, fair utilization, and rational management of water resources in arid and semiarid regions [1–3].

Since water availability in arid regions is both sporadic and variable in intensity, traditional water resources assessment relying on ground-based techniques and data can often lead to poor estimates of key drivers of hydrologic processes [4]. For example, most ground-based rain gauge networks are inadequate to capture spatial and temporal heterogeneity of precipitation [5]. Therefore, conventional hydrological measurements combined with satellite and airborne remote sensors can be useful and cost-effective and for mapping and monitoring water resources. Furthermore, remotely sensed data can be used in large-scale geologic/hydrologic models to simulate hydrologic processes, quantify the spatial and temporal water distribution, and prepare maps of groundwater potential zones [3, 6–8].

A key to remote sensing of groundwater is the realization that shallow groundwater flow is often driven by surface forcing parameterized by geologic properties inferred from surface data [9]. Thus, satellite data is especially effective if it is used with ancillary data analysis to infer groundwater behavior from surface expressions. Groundwater and surface water are closely connected in both arid and humid environments [10]. In arid environments, streams and lakes can be separated from the water table by a large vadose zone. During wet seasons, groundwater may become perched below surface water and then dissipate during dry seasons. Because water typically controls the growth of vegetation in arid areas, an

outcropping of groundwater can usually be identified in remotely sensed images by its vegetative spectral signature. The problem in arid environments is that much of the groundwater flow emerging at the surface is intermittent. Therefore, time series of ground data and multiple remotely sensed images are required to distinguish steady groundwater flow from storm-driven or seasonal behavior [9].

Topographically driven groundwater flow implies that groundwater will be recharged over broad upland areas and discharged at relatively focused lowlands as surface water. In arid areas, evapotranspiration may also play a role. From a remote sensing point of view, water can thus be present in many forms, where each requires a different remote sensing approach in order to be detected and mapped.

Exposed surface water can be mapped using visible, near-infrared and radar imagers. Soil moisture is best measured with microwave radiometers or radar. Vegetation indicating the presence of springs can be mapped with multispectral imagers, while freshwater springs entering water bodies can be detected with thermal infrared (TIR) sensors. Gravitational surveys from satellites have been used to estimate groundwater aquifer storage.

The objective of this chapter is to review the most effective remote sensing techniques for detecting and mapping water resources in arid and semiarid environments. This chapter has been divided into sections addressing application of remote sensing technologies to detecting exposed surface waters, groundwater, soil moisture, freshwater springs, wetlands, and monitoring drought and potential drought conditions in arid and semiarid regions.

2 Identification and Mapping of Arid and Semiarid Regions

Identification and mapping of arid and semiarid regions is a prerequisite for water availability, accessibility, fair utilization, and rational management. Gamo et al. [11] developed a method for classifying arid lands. The objective of that project was to prepare internally consistent maps of arid regions on a global scale in an effort to understand the conditions of existing arid regions, especially deserts and soil degradation areas. They delimited arid regions on a global scale by combining climate data, i.e., aridity index (AI), and vegetation data, i.e., vegetation index (VI). The AI shows the degree of climatic dryness and the VI denotes the abundance of vegetation. The annual AI was estimated by the ratio of mean annual precipitation to mean annual potential evapotranspiration, using the Thornthwaite method. The VI was derived on a global scale in real time from satellite remote sensing images produced by the NASA/NOAA Advanced Very High Resolution Radiometer (AVHRR) visible and near-infrared bands. The long-term mean of yearly maximum normalized difference vegetation index (NDVI) (ymx) was used as an indicator of vegetation condition.

Arid regions of the world were classified by Gamo et al. [11] into four categories:

- Category A, severe deserts, where both aridity and vegetation indices are very small
- Category G, semiarid regions, where the VI is proportionally related to the AI
- Category I, irrigated areas and oases, where the vegetation is relatively abundant despite severe dryness
- Category S, soil degradation areas, where the vegetation is poor despite relatively humid conditions

The standard deviation of NDVI (ymx) is very small for severe deserts and much larger in semiarid areas. Thus, the Sahara desert (Category A) was clearly distinguished from the Sahel; the latter belongs to Category G and drought occurs frequently there between rainy seasons. Desert areas were further classified into severe deserts (Category A), grassland deserts (Category G), and soil degradation deserts (Category S). As a result, a map was produced showing the global distribution of arid regions using these unified criteria with both physical and biological meaning [11].

3 Detecting and Mapping Inland Surface Waters

Surface waters include streams, rivers, ponds, lakes, and other exposed inland water bodies. Remote sensing provides an effective means for mapping the location, extent, and changes of surface water bodies over time [12, 13]. For example, remotely sensed seasonal changes of lake water extent can be combined with available topographic data to estimate water volumetric storage changes and thus more accurately manage water resources [14–16].

A variety of passive and active remote sensors with visible and microwave bands can be used to estimate inundation area and delineate water boundaries [17]. The land–water boundary can be easily defined using the near-infrared radiation (NIR) region of the electromagnetic spectrum. Land appears much brighter than water because water strongly absorbs the NIR. Most multispectral and hyperspectral sensors include suitable NIR bands. Moderate resolution satellites, such as Landsat Thematic Mapper (TM) and SPOT (Satellite Pour l’Observation de la Terre), have been used to study surface water bodies and determine their extent in arid and semiarid regions. For example, Sharma et al. [2] used the Landsat TM to map small surface water bodies in arid areas of India and compared them to Survey of India topographical maps. They found major reductions in areal extent of the water bodies over 28 years, mainly due to cultivation and urbanization in these desert regions. Data from high-resolution commercial satellites, such as IKONOS and QuickBird, have been used to produce more detailed maps of small freshwater areas. Figure 1 shows a high-resolution NIR IKONOS satellite image, containing bogs, lakes, and wetlands in northern Wisconsin, USA.

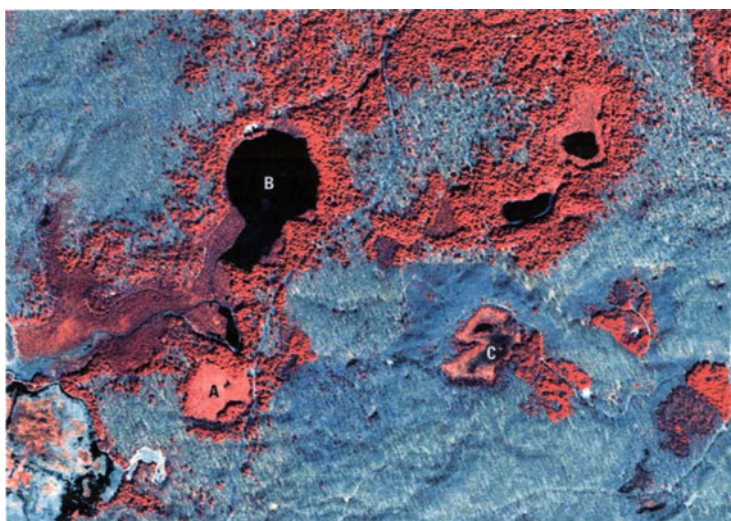


Fig. 1 High-resolution near-infrared IKONOS satellite image of bogs (a), lakes (b), and wetlands (c) of northern Wisconsin, USA, spring 2005. Image courtesy of Space Imaging Corp

In African arid and semiarid regions, rainfall amounts vary drastically within a season and between seasons; as such, surface water availability can radically change. Detecting the change when surface water sites are filled by rainfalls and when they are drained out is key information for the assessment of water availability and environmental conditions, providing alerts on vector-/insect-borne diseases or managing human activities. Combal et al. [18] used the VEGETATION instrument onboard SPOT satellites to detect surface water, using the NIR at a resolution of 1 km over Africa. The surface water was detected every 10 days and broadcast to users by means of the EUMETCast broadcasting system operated by EUMETSAT. EUMETCast is a multiservice dissemination system that uses geostationary satellites to multi-cast data to a wide user community. The detection of surface water coupled with the broadcasting system provided the capacity for operational monitoring of surface water at continental to regional scales. The continuity of surface observations allowed for seasonal assessment of water availability [18].

Where clouds, trees, and other vegetation obscure the water surface, synthetic aperture radar (SAR) can be used to detect surface water. SAR can penetrate clouds to detect standing water through emergent aquatic plants and forest canopies [19]. Water bodies scatter the pulses emitted by radars. Since most SAR sensors use a side-looking antenna, open waters appear dark as the radar pulses are not returned (backscattered) to the radar antenna. If a wet surface is covered by vegetation, the radar pulse bounces between the vegetation and wet surface, and the backscattered return signal will be stronger than if the surface would have been dry [20]. Table 1 shows the characteristics of some typical SAR satellites. Note the good ground resolution and different polarization features. Some newer satellites are also operating in the L-band (15–30 cm) and X-band (2.4–3.75 cm).

Table 1 Overview of synthetic aperture radar (SAR) satellites

Satellite	ERS-1 and ERS-2	RADARSAT	Envisat
Sensor	SAR	SAR	ASAR
Launch dates (s)	July 17, 1991	Nov 4, 1995	Mar 1, 2002
	Apr 20, 1995		
Frequency	5.3 GHz	5.3 GHz	5.3 GHz
Wavelength	5.6 cm	5.6 cm	5.6 cm
Polarization	VV	HH	VV, HH, VH, HV
Incidence angle	20–26°	10–59°	15–45°
Swath width	100 km	50–500 km	100–405 km
Ground resolution	25 × 25 m	8 × 100 m	25 × 25 m

Radar altimetry has been used to obtain point measurements of water surface elevation in order to determine volumetric water storage [16, 21]. For example, Cazenave et al. [22] and Kostianoy et al. [23] report using satellite altimetry data to investigate seasonal, interannual, and space-time variability of the level of water bodies in arid areas of Turkmenistan, including the Caspian Sea water level. They were able to monitor the water level (filling) of the Altyn Asyr Lake since its construction began in July 2009. The synergistic application of combined radar and optical remote sensing was shown to be particularly effective for the analysis of the morphometric characteristics and sea (lake) level of these water bodies.

Airborne bathymetric Lidar has also been used to map water surfaces and to estimate the water volume of lakes by producing elevation models for the water surface and the lake bottom [24, 25]. Some airborne Lidar systems combine near-infrared wavelengths for topography and green wavelengths for bathymetry, allowing water depths to be determined with accuracies of about 10 cm. Bathymetric Lidars can penetrate down to about the equivalent of three Secchi depths and provide bathymetric data down to 6 m depths in lakes of low turbidity.

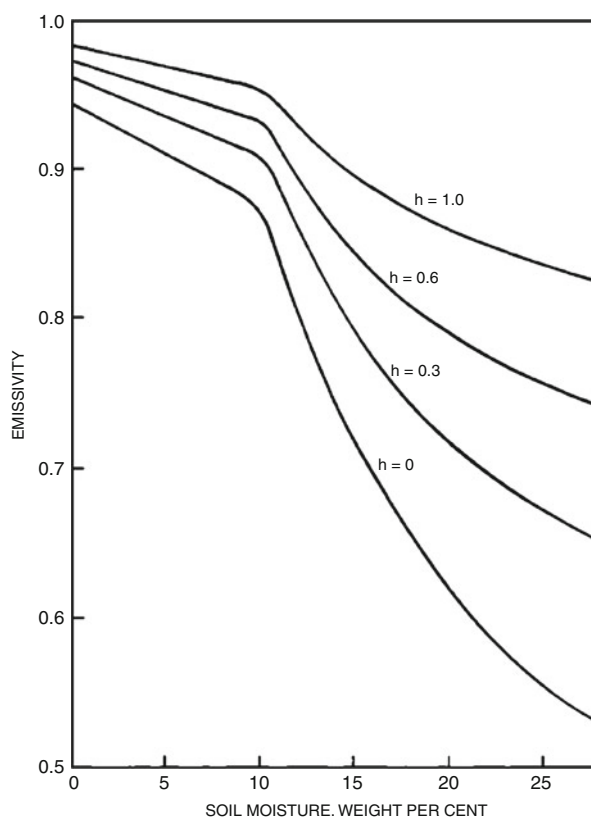
4 Detecting Subsurface Waters

Subsurface water consists of soil moisture (unsaturated or vadose zone) and groundwater aquifer (saturated zone).

4.1 Determining Soil Moisture

Soil moisture is an indicator of subsurface water that is found in the unsaturated zone above the water table. Soil moisture has an important role in the calculation of water and energy budgets needed for climate studies. Soil moisture improves meteorological and climate predictions and is important for assessing agricultural

Fig. 2 Calculated emissivity for a soil using several values of the roughness parameter k . Reprinted from Choudhury et al. [28] with permission from John Wiley and Sons



conditions, irrigation management, and studies of desertification, all of which are especially important in arid and semiarid regions.

Soil moisture also plays a significant role in forecasting arid region droughts. In dry regions of the world, like the Sahel, cloud formation and the rate and distribution of precipitation are partly controlled by the wetness of the soil [26]. The wetness of the terrain influences how much energy it absorbs from the Sun, which in turn affects atmospheric convection, cloud formation, and precipitation. This relationship creates a feedback loop, where rainfall affects the chances of additional precipitation in the days that follow. Thus, a positive feedback would promote floods and drought.

Because microwave radiation is sensitive to soil moisture, microwave remote sensors provide a unique capability for mapping soil moisture over large areas of the Earth's land surface [27]. Both active radars and passive microwave systems can sense soil moisture. Microwave radiometers detect the brightness temperature, which equals the product of the emissivity and the surface temperature of the soil. At frequencies below 5 GHz the emissivity of soils varies over a wide range from about 0.6 for wet, saturated soils to greater than 0.9 for dry soils. Figure 2 shows the strong relationship between soil moisture and emissivity in the 21 cm microwave

band for different values of soil roughness. The microwave radiometer measurement of soil moisture is also affected by the density of any vegetative cover, including grass, shrubs, and trees.

Radars measure the backscattering coefficient, which is a measure of reflectivity. Passive and active methods are related through Kirchhoff's law, $e = 1 - r$, where e is the emissivity and r is the reflectance. Since an increase in soil moisture decreases its emissivity, it simultaneously increases the radar reflectivity or backscatter. Radar is more sensitive to surface roughness and dense vegetation structure than optical sensors but is less affected by surface temperature and provides good spatial resolution.

Early remote sensing of soil moisture was performed from aircraft [29–31]. More recently satellite sensors are numerous and able to provide information on surface soil moisture. Remotely sensed surface soil moisture data sets have been acquired with scatterometer observations of the Active Microwave Instrument (AMI) on the European Remote Sensing satellites (ERS-AMI) and the Advanced Scatterometer (ASCAT) on MetOp. Multifrequency radiometers have also been used, including the Advanced Scanning Microwave Radiometer (AMSR-E), the Scanning Multichannel Microwave Radiometer (SMMR), and the Microwave Imager (TMI) on the Tropical Rainfall Measuring Mission (TRMM). Yet despite the importance of soil moisture information, until recently there have been no projects specifically dedicated to measuring soil moisture globally with adequate temporal or spatial sampling [32–34].

With the launch of microwave radiometers on the Soil Moisture and Ocean Salinity (SMOS) and AQUA satellites, soil moisture (along with other parameters such as sea surface salinity) can now be obtained nearly continuously over a large fraction of the Earth's surface [35, 36]. AQUA is a sister satellite to Terra, the first of the large Earth observation satellites (EOS), launched in 1999 to monitor the "health of the planet," with Terra emphasizing land and AQUA emphasizing water. AQUA and SMOS data are providing information on the moisture content of the soil, vegetation conditions (heavily dependent on water), and on many other aspects of the Earth's climate system.

The L-band 2-D interferometric radiometer on SMOS receives the radiation emitted from the Earth's surface, which then can be related to the moisture content in the first few centimeters of soil over land [36–39]. Microwave measurements are largely unaffected by solar illumination and cloud cover, yet accurate soil moisture estimates are still limited to regions that have either bare soils or low amounts of vegetation cover. In the absence of significant vegetation cover, soil moisture dominates the signal received by a microwave radiometer [40, 41]. The low-frequency microwave range of 1–3 GHz (10–30 cm wavelength) is considered best for soil moisture sensing due to its sensitivity to soil moisture, reduced atmospheric attenuation, and greater vegetation penetration at these longer wavelengths. Since mid-July 2010, SMOS has been delivering images of "brightness temperature" to the science community, which are used to produce global maps of soil moisture every 3 days (along with maps of ocean salinity) averaged over 30 days.

The combined use of satellite data from multispectral and TIR radiometers has also shown promise for the retrieval of latent and sensible heat, as well as surface soil moisture variations. These data are important for monitoring plant growth and productivity, irrigation management, modeling atmospheric and hydrological cycles, and improving the accuracy of weather forecast models.

Blending optical data, passive microwave emissivity, and radar backscatter, the Global Inundation Extent from Multi-Satellite (GIEMS) data set is one of the most comprehensive data sets of surface wetness [12, 13]. GIEMS is a coarse scale data set with about 25 km spatial resolution and monthly time-steps available for almost two decades. Recently both high-resolution SAR data [42] and optical images from the MODIS imagery [43] have been used for downscaling GIEMS.

Detecting water in arid regions by means of soil moisture remote sensing still faces many challenges. The spatial resolution over land needs to be improved. As stated earlier, accurate soil moisture estimates are limited to regions that have either bare soils or low amounts of vegetation cover. Better corrections for surface roughness, vegetation cover, soil temperature, and topography must be devised. Until recently, the moisture in only the top few centimeters of the soil could be detected. The Soil Moisture Active Passive (SMAP) satellite mission, planned for the 2015–2020 time frame, is designed to use advanced modeling and data assimilation to provide data on deeper root-zone soil moisture and net ecosystem exchange of carbon [44, 45].

4.2 *Detecting Groundwater*

Groundwater accounts for about 98 % of the total freshwater budget on Earth. The remaining 2 % is divided between rivers, lakes, freshwater wetlands, and moisture in the atmosphere. Groundwater supplies about 40 % of the drinking water in the USA and 70 % in China and is the main source of domestic water supply in most European countries [46]. Groundwater exists within the matrix of sedimentary rocks, occupying pore spaces between sediment grains, housed within rock fractures, or held within large underground caverns [10, 47].

Shallow-layer groundwater within a few centimeters of the surface may be detected by SAR microwave radiometry or TIR imagery in certain geologic settings [48]. However, groundwater aquifers located deep below the land surface cannot be detected directly by electromagnetic remote sensors and are usually surveyed with gravitational techniques. Groundwater discharges to the surface via springs that feed rivers, lakes, and wetlands and can be mapped by many different remote sensing systems, as described in later sections of this chapter. In arid environments, the surface discharge of groundwater may also be indirectly detected by remote sensing, if the discharge produces areas of unusually dense vegetation [49].

High-resolution gravitational surveys have been used to estimate groundwater storage [50, 51]. However, gravitational instruments have no vertical resolving power, so that measurement of subsurface water pools requires removing the

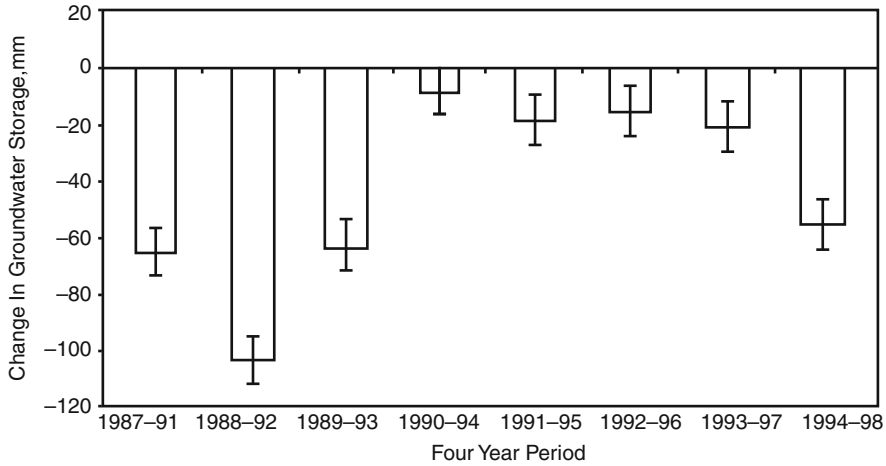


Fig. 3 Four-year changes in the central USA. High Plains aquifer water storage with error bars that represent the total uncertainty in GRACE-derived estimates. Reprinted from Rodell and Famiglietti [54] with permission from Elsevier

influence of water stored in the unsaturated soil zone. For aerial surveys, corrections must also be made for water stored in vegetation. For satellite gravity surveys, one must correct the water effects of the atmosphere in addition to the vegetation.

At present, there is only one satellite mission that can directly estimate the quantity of groundwater stored deep beneath the Earth's surface. It accomplishes this by measuring the Earth's gravity field which is influenced by the quantity of groundwater below the surface. As groundwater is consumed or recharged, water-induced gravity anomalies change through time. The Gravity Recovery and Climate Experiment (GRACE) mission, launched in 2002, consists of two identical satellites orbiting in unison at the same altitude but with a separation of 220 km. The two satellites monitor the relative position of each other using microwave-ranging instruments. As they pass over a gravity anomaly, the leading spacecraft approaches and speeds up due to higher angular momentum. This causes the two satellites to increase separation. After the first spacecraft passes the anomaly, it slows down again; meanwhile the following satellite accelerates, then decelerates over the same point. By recording satellite separation, gravity is mapped; cycles of growing/shrinking separation indicate the size and strength of the gravity anomalies, from which the quantity of groundwater can be estimated [49].

Due to atmospheric variability and observational errors, accurate estimates of water mass can only be obtained for regions that are several hundreds of kilometers or more in scale [52]. Thus, estimating water storage changes in large aquifer systems is currently feasible [53]. Rodell and Famiglietti [54] used computer simulations and GRACE performance parameters to show that groundwater storage changes as small as 9 mm could be measured in the US High Plains aquifer system. As shown in Fig. 3, in the High Plains the magnitude of annual groundwater storage changes averaged 19.8 mm between 1987 and 1998. They expected that the

uncertainty in deriving estimates of aquifer storage changes from GRACE observations would arise mainly from the removal, via land surface modeling, of the effects of soil moisture changes from the gravity signal. Rodell and Famiglietti [54] were predicting the total uncertainty to be about 8.7 mm. Comparing the 4-year groundwater storage change bars with the estimated GRACE uncertainty bars in Fig. 3, one can see that such estimates would have been useful for tracking groundwater changes in the High Plains aquifer during most 4-year periods.

Yirdaw et al. [55] investigated the Canadian Prairie drought by employing total water storage anomalies obtained from the GRACE remote sensing satellite mission. The obtained GRACE-based total water storages were validated using storages estimated from the atmospheric-based water balance P-E (precipitation-evaporation) computation in conjunction with measured streamflow records. The results from their study corroborated the potential of the GRACE-based technique as a useful tool for the characterization of the 2002/2003 Canadian Prairie droughts.

Li et al. [56] assimilated anomalies of terrestrial water storage (TWS) observed by the GRACE satellite mission into the NASA Catchment land surface model in western and central Europe for a 7-year period. GRACE data assimilation led to improved runoff estimates (in temporal correlation and root mean square error) even in basins smaller than the effective resolution of GRACE. Signals of drought in GRACE TWS correlated well with the MODIS NDVI in most areas. Although they detected the same droughts during warm seasons, drought signatures in GRACE-derived TWS exhibited greater persistence than those in NDVI throughout all seasons, in part due to limitations associated with the seasonality of vegetation [56].

To derive estimates of aquifer storage changes from GRACE observations, one faces the challenge of removing the effects of soil moisture changes from the gravity signal by means of land surface modeling. Plans for a follow-on mission to GRACE may result in groundwater storage estimates that are more accurate and of greater relevance to typical large aquifer systems [57]. The GRACE follow-on mission is scheduled for 2017 and would re-fly the identical GRACE spacecraft and instruments but supplement the micrometer-level accuracy microwave measurement with a laser interferometer with nanometer-level accuracy.

Models are being developed to identify groundwater potential zones [6–8]. For example, Asadi et al. [1] have performed a model study for sites in the Hyderabad and other districts of India, which identifies groundwater potential zones using IRS-ID PAN and LISS-III satellite geocoded data on a 1:50,000 scale. The information from base maps, drainage maps, watershed maps, geomorphology maps, groundwater table maps, and groundwater infiltration maps were used as data layers in a GIS to prepare a database. Then the relationships between the GIS data layers were analyzed and integrated to prepare the groundwater potential zones map.

Machiwal et al. [58] used ten thematic layers in a GIS, including data obtained by remote sensing, and multi-criteria decision-making techniques (MCDM) to delineate groundwater potential zones in the Udaipur district of Rajasthan, India. The GIS layers included topographic elevation, land slope, geomorphology, geology, soil type, pre- and post-monsoon groundwater water depths, annual net

recharge, annual rainfall, and proximity to surface water bodies. These thematic layers were studied by principal component analysis techniques to select the most influential layers for groundwater prospecting. Seven thematic layers were selected, and their features were assigned suitable weights according to their relative importance with regard to groundwater occurrence. The selected thematic maps were integrated by weighted linear combination methods in a GIS environment to generate the groundwater potential maps [58].

A recent example of successfully combining traditional geology and cutting-edge digital tools to reveal underground aquifers in drought-stricken areas is described by Gramling [59]. Accordingly, a scientific team led by geologist Alain Gachet, head of Radar Technologies International (RTI), found large water aquifers in northwestern Kenya where a drought was devastating the land, causing crops to collapse, livestock to die, and prompting a food crisis that affected millions of inhabitants in Kenya, Somalia, South Sudan, and Ethiopia. The team is part of the UNESCO Groundwater Resources Investigation for Drought Mitigation in Africa Program.

The area explored by Gachet's team, Turkana County, Kenya, is bordered in the east by Lake Turkana, a water-filled depression that is part of the East African Rift, a region having a stretched and fractured crust. Between the fractures, sunken blocks of land called grabens form sediment-filled troughs that are several kilometers deep. The troughs were a primary target, because they are potential traps for groundwater. To identify them, RTI used powerful computer programs to merge refined geological knowledge with large samples of data from ground sensors and space-based remote sensors. The data used included traditional geologic maps, hydrologic data, satellite images, and gravity and seismic survey data. Gachet's team also used commercial satellite radar images to detect soil moisture. RTI developed image-processing technology, WATEX, which "erases" obstacles, such as rocks and villages that can obscure the images, to reveal traces of moisture that can suggest the presence of an aquifer. WATEX helped identify five likely aquifers under the desert, each more than 100 m below the surface, containing water resources totaling at least 250 billion cubic meters. So far, drilling has confirmed existence of two of the aquifers. The RTI team expects to find many more deeply buried groundwater aquifers in arid regions, such as South Sudan and Sudan's Darfur state [59].

5 Detecting Freshwater Springs and Biomass

Freshwater springs can occur on dry land, in wetlands, and along the coast. Springs occur when groundwater is confined by a low-permeability geologic formation, which constrains water to a focused discharge point. Fractures in hard rock and confining clay units are typical conduits for spring flow [60]. Springs may discharge at the land surface or below the open water surface. In arid areas, freshwater springs and irrigated areas induce the growth of a dense vegetation cover, including trees,

shrubs, or grasses. Detecting biomass production is a common approach used to identify the presence of freshwater springs.

5.1 Detecting Freshwater Plumes

Where groundwater enters a lake or coastal waters, it may display a thermal, chemical, or vegetation signature that can be sensed remotely. To detect and map freshwater plumes, remote sensors exploit differences in temperature, salinity, turbidity, or color from ambient background water [61, 62]. Groundwater discharges in submarine springs have been detected using airborne and satellite TIR sensors [63, 64]. Thermal anomalies on beaches or in coastal waters are often associated with freshwater springs.

In the United Arab Emirates, a critical shortage of water is the limiting factor in municipal, industrial, and agricultural development. Most of the precipitation of up to 400 mm falls in some of the higher mountainous areas and much of it infiltrates into the ground. Thomson and Nielsen [65] did a study to determine to what extent this water was infiltrating into the sea and was therefore lost to human use and where such losses were occurring. The period of February to March was considered the best time of the year to conduct an airborne TIR study for locating springs, since the sea surface temperatures were at a minimum during this time of the year. Two flights were conducted in the early morning to minimize effects of surface heating by the sun and to take advantage of low tide conditions [66]. The sea state was moderate and winds were light during both flights. Coincident with the airborne data, surface temperatures of several different materials were measured at a number of locations along the coast, including asphalt roads, sand, etc. Aerial photos at a scale of 1:60,000 were also analyzed to aid in the identification of possible groundwater discharge sites. At the time of the airborne data collection, groundwater temperatures were about 13 °C higher than the sea surface temperature, and any groundwater discharges would appear warmer than the surrounding sea water. Colder discharges would indicate surface runoff from recent storms. Analysis of the thermal imagery indicated eight possible areas of groundwater discharge which were pinpointed on a topographic map and each identified with the name of the nearest village [65]. All groundwater discharges occurred at the shoreline-seawater interface, and no offshore springs were detected.

Groundwater discharges are usually not uniformly distributed but are strongest near the shoreline and decrease exponentially away from the shoreline. The spatial distribution of spring discharges into streams, bays, and lakes has been studied using TIR and multispectral sensors on aircraft and satellites [9]. Multi-beam sonar has also been used to characterize submarine freshwater springs down to depths of tens of meters [67].

Fig. 4 True color Terra MODIS image from August 23, 2003 of the Nile River Valley with snakes in a vegetated green line from Lake Nasser in southern Egypt to the edge of the Mediterranean Sea, where it widens out into a highly productive, vast delta. *Credits: NASA*



5.2 *Determining Biomass Production*

Figure 4 shows a Terra MODIS image of the Nile River, which brings much-needed water and silt to the Nile Valley, turning it into an oasis of agriculture and life. The reason that the Nile River and some of the oases in Egypt are highly visible in this image is because the river and springwater irrigate the soil and produce dense vegetation that contrasts strongly with the surrounding arid land. At the apex of the delta is Cairo, which appears as a gray-brown spot. The leaf-shaped patch of green branching off the western side of the Nile is a depression that has been used as irrigated agricultural area since 1800 BC.

Arid areas generally have sparse vegetation showing little biomass production. However, where a freshwater spring emerges, biomass production is usually much higher than normal. Aboveground biomass is usually evaluated by using one of several vegetation indices [68, 69]. The most common index used is the NDVI, which is expressed as the difference between the red and NIR reflectances divided

by their sum [70, 71]. These two spectral bands represent the most detectable spectral characteristics of green plants. This is because the red radiation is absorbed by the chlorophyll in the surface layers of the plant (*palisade parenchyma*) and the NIR is reflected from the inner leaf cell structure (*spongy mesophyll*) as it penetrates several leaf layers in a canopy. Since the NIR reflectance depends on the abundance of plant tissue and the red reflectance indicates the leaf surface health condition of the plant, the NDVI can be related to plant biomass or stress. It has been shown by researchers that time series of remote sensing data can be used effectively to identify long-term trends and subtle changes of NDVI by means of principal component analysis [68, 72, 73]. However, the NDVI must be used with caution in areas with less than 20 % vegetation cover because the vegetation spectra will be distorted by the soil reflectance. Care must also be used in areas where the vegetation fraction is higher than 50 % and the signal is pushed into the saturated region of the nonlinear transfer curve.

Visible, infrared, and microwave sensors have varying sensitivities to above-ground vegetation biomass. Optical and radar remote sensing methods and empirical and statistical regression models, some using NDVI, have been applied to estimate the amount and variability of aboveground biomass [74–78]. Remote sensing has been used to collect large amounts of biomass data on a global scale for forested areas, such as upland forests, forested wetlands, and mangroves [79]. Extensive work is under way with L-band SAR to develop operational biomass programs across a range of countries, using an approach that is effective over a biomass range of 0–200 tons/ha [80].

5.3 Biomass as a Drought Indicator

Drought is a gradual phenomenon, slowly taking hold of an area and stressing its vegetation. In severe cases, drought can last for many years with devastating effects on agriculture and water supplies. The underlying cause of most droughts, deficiency in precipitation, can be related to variations in large-scale atmospheric circulation patterns and the locations of anticyclones, or high pressure systems. Sometimes, whirling masses of air separate from the main westerly airflow and effectively prevent the usual west to east progression of weather systems. When these “blocking systems” persist for extended periods of time, weather extremes such as drought, floods, heat waves, and cold snaps can occur [81].

One of the worst droughts of the twentieth century occurred in the Horn of Africa in 1984 and 1985. Figure 5 shows the NDVI anomaly for August 1984. Within this figure, dark red/brown indicates the most severe drought, light yellow areas are normal, and green areas have denser than normal vegetation. This figure demonstrates the widespread areas of severe drought that can be mapped using remote sensing techniques.

The NDVI anomaly indicates the vigor of vegetation relative to the long-term average. Using NOAA’s AVHRR, scientists have been collecting images of the

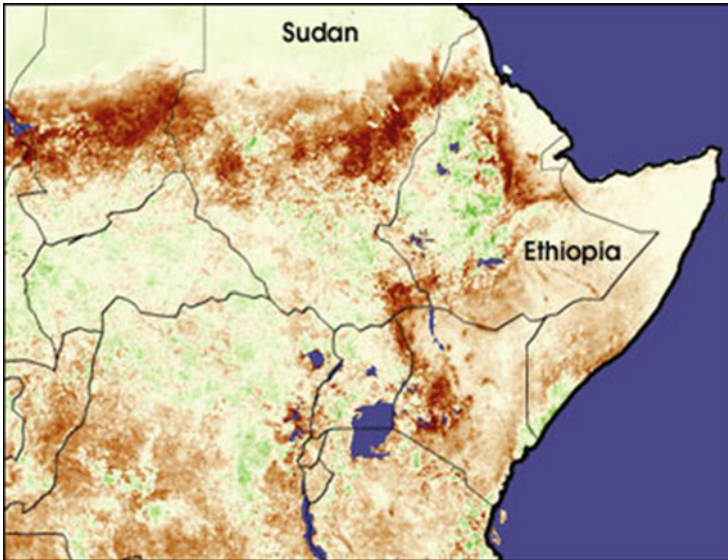


Fig. 5 This image shows the Normalized Difference Vegetation Index (NDVI) anomaly of the Horn of Africa for August 1984. The NDVI anomaly indicates the vigor of vegetation relative to the long-term average. *Dark red/brown* indicates the most severe drought, *light yellow* areas are normal, and *green* areas have denser than normal vegetation. *Courtesy: NOAA National Weather Service*

Earth's surface. By carefully measuring the wavelengths and intensity of visible and near-infrared light reflected by the land surface back up into space, scientists use the "Vegetation Index" (NDVI) to quantify the concentrations of green leaf vegetation around the globe [82]. Then by combining the daily Vegetation Indices into 8-, 16-, or 30-day composites, scientists create detailed maps of the Earth's green vegetation density that identify where plants are thriving and where they are under stress (i.e., due to lack of water). To obtain the NDVI values for vegetation biomass or stress studies in smaller areas, higher resolution satellite systems, such as Landsat TM or SPOT, are being used [69].

6 Detecting and Mapping Wetlands

Freshwater wetlands include bottomland hardwoods, riparian forests, bogs, vernal pools, and emergent marshes.

Freshwater wetlands greatly influence water quality, increase detention times of floodwaters, provide habitat for wildlife, serve as spawning and nursery grounds for fish, and contribute to the aquatic food chain [85, 86]. Wetlands also provide flood protection, protection from storm and wave damage, water quality improvement through filtering of agricultural and industrial waste, and recharge of aquifers

[4]. Freshwater wetlands can be an important source of groundwater recharge and water in arid and semiarid areas [87]. However, wetlands have been exposed to a wide range of stress-inducing alterations, including dredge and fill operations, hydrologic modifications, pollutant runoff, eutrophication, impoundments, and fragmentation by roads and ditches.

For more than three decades, remote sensing techniques have been used effectively to detect, map, and monitor tidal wetlands [88–92]. For instance, the US Fish and Wildlife Service (FWS) through its National Wetlands Inventory has provided federal and state agencies and the private sector with scientific data on wetlands location, extent, status, and trends. To accomplish this important task, FWS has used multiple sources of aircraft and satellite imagery and on-the-ground observations [92]. Most states have also created a wide range of tidal wetland inventories, using both aircraft and satellite imagery. The aircraft imagery frequently included natural color and color infrared images. The satellite data consisted of both high-resolution (1–4 m) and medium-resolution (10–30 m) multispectral imagery.

The Landsat TM has been a reliable source for land cover data [93]. Its 30 m resolution and spectral bands have proven adequate for observing land cover changes over large areas (e.g., the Horn of Africa). Freshwater wetlands have been mapped using Landsat TM and other medium-resolution data [94–97]. The availability of high spatial resolution (0.4–4.0 m) satellite data has significantly improved the capacity for mapping isolated and upstream freshwater wetlands [89, 98, 99]. However, the cost per sq. km. of imagery and its analysis increases very rapidly from using medium-resolution to high-resolution imagery. Therefore, large wetland areas or entire watersheds should be mapped using medium-resolution sensors, such as Landsat TM at 30 m, and only small, critical areas should be examined with high-resolution sensors, such as IKONOS at 1–4 m resolution [98].

Airborne geo-referenced digital cameras providing color and color infrared digital imagery are particularly suitable for accurate mapping of small freshwater wetland sites or interpreting satellite data. For example, in Fig. 6, the wetlands map shown on the left was derived from an airborne ADS-40 digital camera image shown on the right. At a spatial resolution of 0.5 m, the ADS-40 digital imagery was able to identify three key species of marsh vegetation (i.e., *Phragmites*, *Typha*, and *Spartina*). Digital cameras are often used on small aircraft flown at low altitudes (e.g., 200–500 m) and can be used to guide and supplement field data collection [98, 100]. Most digital cameras are capable of recording reflected visible to near-infrared light. In some cases digital camera spectral bands can be matched with specific satellite imaging band, e.g., blue, green, red, and near-infrared bands matching the bands of the IKONOS satellite multispectral imager [101]. Digital camera imagery can be integrated with GPS information and used with geographic information system software for a wide range of modeling applications [102].

Groundwater discharges in wetlands can also be identified by the unique vegetation species they may support. For example, in *Spartina alterniflora* tidal marshes groundwater discharges have been identified because they decrease the local salinity and thus attract other species to grow, such as invasive *Phragmites australis*

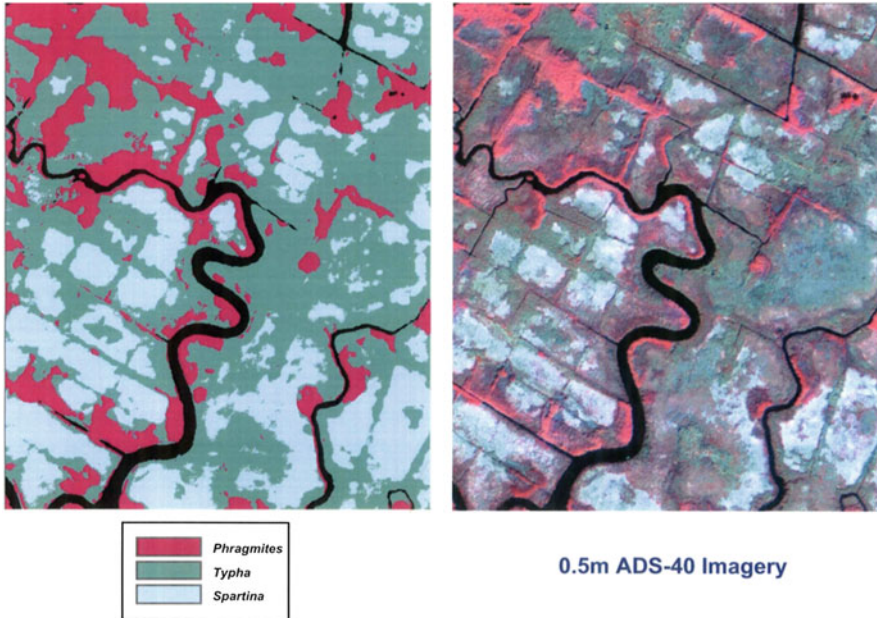


Fig. 6 The wetlands map shown on the *left* was derived from an airborne ADS-40 digital camera image on the *right*. Note that three different marsh vegetation species were identified. *Credits:* NOAA National Ocean Service, Charleston, SC, USA

[103]. Since most freshwater discharges in wetlands and in shallow waters are small, high spatial resolution remote sensors must be used to detect them.

New advanced techniques have been developed for mapping wetlands and even identifying wetland types and plant species indicating the presence of water [91, 98, 104–107]. The integration of hyperspectral imagery and Lidar-derived elevation has also significantly improved the accuracy of mapping wetland vegetation. Hyperspectral images help distinguish wetland species, and the Lidar data help separate species by their height [108]. Major plant species within a complex, heterogeneous wetland have been classified using multi-temporal high-resolution QuickBird satellite images, field reflectance spectra, and Lidar height information [109]. Using Lidar, hyperspectral and radar imagery, and narrow-band vegetation indices, researchers can discriminate between some wetland species and also estimate biochemical and biophysical parameters of wetland vegetation, such as water content, biomass, and leaf area index [69, 109–112].

SAR sensors on satellites provide the increased spatial resolution that is necessary in regional wetland mapping. SAR data have been used extensively for this purpose [113–118].

The sensitivity of microwaves to water and their ability to penetrate vegetative canopies make SAR also ideal for the detection of hydrologic features below the vegetation [119–125]. The presence of standing water interacts with the radar signal

differently depending on the dominant vegetation type/structure [20] as well as the biomass and condition of vegetation [126, 127]. In areas of open water without vegetation, specular reflection occurs and a dark signal (weak or no return) is observed [128]. Specular reflectance also occurs in wetlands dominated by lower biomass herbaceous vegetation when a layer of water is present [129]. Conversely, the radar signal is often increased in forested wetlands when standing water, such as flooding, is present due to the double-bounce effect, i.e., the radar pulse is reflected strongly by the water surface away from the sensor (specular reflectance) but is then redirected back towards the sensor by a second reflection from a nearby tree trunk [128, 130].

Wetland InSAR is a unique application of the interferometric synthetic aperture radar (InSAR) technique that detects elevation changes of aquatic surfaces. Most other InSAR applications detect displacements of solid surfaces [131]. The technique works because the radar pulse is backscattered twice (double bounce) from the water surface and vegetation. Wetland InSAR provides high spatial resolution hydrologic observations of wetlands and floodplains that cannot be obtained by any terrestrial-based methods. InSAR observations of wetlands have been acquired over various wetland environments using L-, C-, and X-bands and different polarizations [132, 133]. L-band data are most suitable for the wetland InSAR applications. However, the X- and C-band radar signals, which primarily interact only with the upper sections of the vegetation, were also found to be useful. In general, promising applications of InSAR for wetland observations include high spatial resolution water level monitoring, detection of flow patterns and flow discontinuities, and constraining high-resolution flow models [131].

7 Drought Monitoring and Prediction

Accurate mapping and monitoring of drought severity is important for water management and drought mitigation efforts. A system for drought monitoring and prediction can be a vital tool to facilitate drought response while saving money, time, and lives [134]. Drought indicators can be based on one variable or a combination of variables. Different indicators describe various aspects of droughts; however, holistic, comprehensive drought assessment requires multiple indicators. Drought indices integrate large amounts of data, such as precipitation, vegetation condition, snowpack, streamflow, and other water presence/supply indicators, to monitor drought severity in a comprehensive framework and to measure how much the climate in a given period has deviated from historically established normal conditions [135, 136]. These indicators can be obtained from different sources, including satellite observations, model simulations, and reanalysis of past data.

One example of a system for monitoring and predicting drought is the Global Integrated Drought Monitoring and Prediction System (GIDMaPS) developed in 2012 by researchers at the University of California, Irvine [83]. The system gathers and synthesizes land-atmosphere model simulations and remote sensing

observations to generate 1- to 4-month drought predictions. The system helps farmers, commodity investors, local governments, and global relief organizations plan for and react to droughts [84].

GIDMaPS is designed as a cyber-infrastructure system to facilitate drought analysis based on multiple indicators and input data sets. The system can support advanced data management, acquisition, storage, and visualization. The system integrates data from multiple institutions and provides historical and near-real-time drought conditions as well as probabilistic future forecasts [83]. Currently the monitoring and prediction information are based on three indicators: standardized precipitation index (SPI) as a measure of meteorological drought, standardized soil moisture index (SSI) as indicator of agricultural drought, and the multivariate standardized drought index as a composite agro-meteorological drought index. From the main interface, users can select the input data, drought indicator, year, and month to visualize or download drought information [84]. Other investigators have been able to predict agricultural drought through the prediction of agricultural yield using models based on the SPI and the NDVI [137].

Recent advances in remote sensing from satellites and radar, as well as the use of thousands of daily in situ precipitation measurements, have significantly improved drought monitoring capabilities [138]. Significant advances in mitigating drought impacts have also been made by forecasting the conditions that result in drought. Meteorologists at the NOAA Climate Prediction Center (CPC) are using medium-range forecast models to predict soil moisture 2 weeks into the future. For the longer term, meteorologists are using statistical techniques and historical drought information to construct analogues to current conditions. They then create forecasts up to several seasons ahead of time based on past events. CPC is also using sophisticated computer models that link ground and ocean conditions to the overlying atmosphere to create forecasts of temperature, precipitation, and soil moisture months in advance [138].

8 Conclusions

In arid and semiarid environments, the exploration, detection, mapping, and monitoring of water resources are a prerequisite for freshwater availability, accessibility, fair utilization, and rational management. Arid lands, including soil degradation and irrigated areas, have been classified based on vegetation and aridity indices using remotely sensed data. The arid regions have been delimited on a global scale by combining climate data, i.e., aridity index (AI), and vegetation data, i.e., vegetation index. Maps of the global distribution of arid regions have been produced using these unified criteria that have both physical and biological meaning. To monitor and predict droughts, systems exist that use multiple drought indicators to allow users to visualize and download drought information. Significant advances in mitigating drought impacts have also been made by forecasting the conditions that result in drought.

Satellite and airborne remote sensing has proven to be a relatively cost-effective and useful approach for detecting, mapping, and monitoring surface and subsurface water as compared to conventional hydrological methods. Moderate resolution satellites, such as Landsat TM and SPOT, and high-resolution satellites, such as IKONOS and QuickBird, have been used to study surface water bodies and determine their extent in arid and semiarid regions. Remotely sensed seasonal changes of lake water area/extent can be combined with available topographic data to estimate water volumetric storage changes. Where clouds, trees, and other vegetation obscure the water surface, SAR is being used, since it can penetrate clouds and vegetation to detect standing water. Radar altimetry has been applied to obtain point measurements of water surface elevation in order to determine volumetric water storage.

Soil moisture is an indicator of subsurface water that is found in the unsaturated zone above the water table. Soil moisture information is required to improve meteorological and climate predictions and for assessing agricultural conditions, irrigation management, hydrologic problems, and studies of desertification. Both active radars and passive microwave systems can sense soil moisture. However, soil moisture remote sensing still faces many challenges: the spatial resolution over land needs improvement, accurate soil moisture estimates are limited to regions with either bare soils or low amounts of vegetation cover, and better corrections for surface roughness, vegetation cover, soil temperature, and topography must be devised. Until recently, the moisture in only the top few centimeters of the soil could be detected. The SMAP satellite mission, planned for the 2015–2020 time frame, is designed to use advanced modeling and data assimilation to provide information on deeper root-zone soil moisture.

To identify groundwater potential zones, powerful computer programs are being developed to merge refined geological knowledge with large samples of data from ground sensors and space-based remote sensors. The data used include traditional geologic maps, hydrologic data, satellite images, and gravity and seismic survey data. Thematic layers in a GIS, including remote sensing data, and multi-criteria decision-making (MCDM) techniques are being used to delineate groundwater potential zones. The selected thematic maps can then be integrated by weighted linear combination methods in a GIS environment to generate the groundwater potential maps.

Only one satellite mission can directly estimate/measure the quantity of groundwater stored deep beneath the Earth's surface. The GRACE mission accomplishes this by measuring the Earth's gravity field which is influenced by the quantity of groundwater below the surface.

Freshwater springs can occur on dry land, in wetlands, and along the coast. Springs may discharge at the land surface or below the water surface. In arid areas, freshwater springs and irrigated areas induce the growth of a dense vegetation cover, including trees, shrubs, or grasses. Vegetated areas can be detected by remote sensors on aircraft and satellites and thus help find locations of freshwater springs.

Freshwater wetlands can be an important source of groundwater recharge and water in arid and semiarid areas. High spatial resolution (0.6–4.0 m) satellite and airborne hyperspectral sensors have significantly improved the capacity for mapping freshwater wetlands. However, the cost per sq. km. of imagery and the accompanying analysis rises very rapidly as one goes from medium-resolution (e.g., 30 m) to high-resolution imagery. Airborne geo-referenced digital cameras are particularly suitable for mapping small freshwater wetland sites. To detect changes of water level in wetlands, InSAR is being used. InSAR provides high spatial resolution hydrologic observations of wetlands and floodplains that cannot be obtained by any terrestrial-based methods.

Airborne and satellite remote sensors are showing considerable promise for detecting, mapping, and monitoring surface water, soil moisture, freshwater springs, and associated vegetation in arid and semiarid regions of the Earth. Satellite-based remote sensing of groundwater is still an unresolved problem. At present, the best that can be achieved with satellite sensors is to determine the spatial distribution of groundwater discharge and recharge areas, storage changes over large areas, or measurement of surface water heads in large water bodies. Combining satellite measurements with physically based models seems to offer renewed hope for detecting groundwater aquifers.

References

1. Asadi SS, Rani N, Vasanth Rao BVT, Raju MV (2012) Estimation of groundwater potential zones using remote sensing and GIS: a model study. *Int J Adv Sci Res Tech* 2:265–275
2. Sharma KD, Singh S, Singh N, Kalla AK (1989) Role of satellite remote sensing for monitoring of surface water resources in an arid environment. *Hydrol Sci J* 34:531–537
3. Yan E, Milewski A, Sultan M, Abdeldayem A, Soliman F, Abdel Gelil K (2010) Remote sensing based approach to improve regional estimation of renewable water resources for sustainable development. In: *Proceedings of US-Egypt workshop on space technology and geo-information for sustainable development*, Cairo, Egypt, 14–17 June 2010
4. Odum EP (1993) *Ecology and our endangered life-support systems*, 2nd edn. Sinauer, Sunderland, p 320
5. Krajewski WF, Smith JA (2002) Radar hydrology: rainfall estimation. *Adv Water Resour* 25:1387–1394
6. Jha MK, Chowdhury A, Chowdary VM, Peiffer S (2007) Groundwater management and development by integrated remote sensing and geographic information systems: prospects and constraints. *Water Resour Manag* 21:427–467
7. Sener E, Davraz A, Ozelcik M (2005) An integration of GIS and remote sensing in groundwater investigations: a case study in Burdur, Turkey. *Hydrogeol J* 13:826–834
8. Solomon S, Quiel F (2006) Groundwater study using remote sensing and geographic information systems (GIS) in the central highlands of Eritrea. *Hydrogeol J* 14:1029–1041
9. Becker MW (2006) Potential for satellite remote sensing of ground water. *Ground Water* 44:306–318
10. Brutsaert W (2005) *Hydrology: an introduction*. Cambridge University Press, Cambridge, p 605
11. Gamo M, Shinoda M, Maeda T (2013) Classification of arid lands, including soil degradation and irrigated areas, based on vegetation and aridity indices. *Int J Remote Sens* 34:6701–6722

12. Papa F, Prigent C, Aires F, Jimenez C, Rossow WB, Matthews E (2010) Interannual variability of surface water extent at the global scale, 1993–2004. *J Geophys Res* 115 (D12):D12111
13. Prigent C, Papa F, Aires F, Rossow WB, Matthews E (2007) Global inundation dynamics inferred from multiple satellite observations, 1993–2000. *J Geophys Res* 112(D12):D12107
14. Frappart F, Papa F, Famiglietti JS, Prigent C, Rossow WB, Seyler F (2008) Interannual variations of river water storage from a multiple satellite approach: a case study for the Rio Negro River Basin. *J Geophys Res* 113:D21104. doi:[10.1029/2007JD009438](https://doi.org/10.1029/2007JD009438)
15. Frappart F, Papa F, Güntner A, Werth S, Ramilien G, Prigent C, Rossow WB, Bonnet MP (2010) Interannual variations of the terrestrial water storage in the Lower Ob' Basin from a multisatellite approach. *Hydrol Earth Syst Sci* 14(12):2443–2453
16. Smith LC, Pavelsky TM (2009) Remote sensing of volumetric storage changes in lakes. *Earth Surf Proc Land* 34:1353–1358
17. Alsdorf DE, Rodríguez E, Lettenmaier DP (2007) Measuring surface water from space. *Rev Geophys* 45:RG2002. doi:[10.1029/2006RG000197](https://doi.org/10.1029/2006RG000197)
18. Combal B, Haas E, Andigue J, Nonguierma A, Bartholome E (2009) Operational monitoring of water bodies in arid and semi-arid regions with SPOT-VEGETATION satellite: contribution of Eumetcast and recent research projects. *Secheresse* 20:48–56
19. Smith LC (1997) Satellite remote sensing of river inundation area, stage, and discharge: a review. *Hydrol Process* 11:1427–1439
20. Hess L, Melack J, Simonett D (1990) Radar detection of flooding beneath the forest canopy: a review. *Int J Remote Sens* 11:1313–1325
21. Calmant S, Seyler F, Cretaux JF (2008) Monitoring continental surface waters by satellite altimetry. *Surv Geophys* 29(4–5):247–269. doi:[10.1007/s10712-008-9051-1](https://doi.org/10.1007/s10712-008-9051-1)
22. Cazenave A, Bonnefond P, Dominh K, Schaeffer P (1997) Caspian sea level from TOPEX-POSEIDON altimetry: level now falling. *Geophys Res Lett* 24:881–884
23. Kostianoy AG, Lebedev SA, Solovyov AM (2011) Satellite monitoring of water resources in Turkmenistan. In: Fifteenth international water technology conference, IWTC-15, Alexandria, Egypt, 31 March–02 April 2011
24. Hofle B, Vetter M, Pfeiffer N, Mandlbürger G, Stotter J (2009) Water surface mapping from airborne laser scanning using signal intensity and elevation data. *Earth Surf Proc Land* 34:1635–1649
25. Paine JG, Andrews JR, Saylam K, Tremblay TA, Averett AR, Caudle TL, Meyer T, Young MH (2013) Airborne lidar on the Alaskan North Slope: wetlands mapping, lake volumes, and permafrost features. *Lead Edge* 32:798–805
26. Schultz C (2014) Spatial resolution key to properly forecasting arid-region drought. *Eos* 95 (13):116
27. Calvet JC, Wigneron JP, Walker JP, Karbou F, Chanzy A, Albergel C (2011) Sensitivity of passive microwave observations to soil moisture and vegetation water content: L-band to W-band. *IEEE Trans Geosci Remote Sens* 49:1190–1199
28. Choudhury BJ, Schmugge TJ, Chang A, Newton RW (1979) Effect of surface roughness on the microwave emission from soils. *J Geophys Res* 81:3660–3666
29. Chanzy A, Schmugge TJ, Calvet JC, Kerr Y, van Oevelen P, Grosjean O, Wang JR (1997) Airborne microwave radiometry on a semi-arid area during HAPEX-Sahel. *J Hydrol* 188–189:285–309
30. Jackson TJ, LeVine DM, Hsu AY, Oldak A, Starks PJ, Isham JD, Haken M (1999) Soil moisture mapping at regional scales using microwave radiometry: the Southern Great Plains Hydrology Experiment. *IEEE Trans Geosci Remote Sens* 37:2136–2150
31. John B (1992) Soil moisture detection with airborne passive and active microwave sensors. *Int J Remote Sens* 13:481–491
32. Barre HJM, Duesmann B, Kerr YH (2008) SMOS: the mission and the system. *IEEE Trans Geosci Remote Sens* 46:587–593

33. Kerr YH, Waldteufel P, Wigneron JP, Martinuzzi JM, Font J, Berger M (2001) Soil moisture retrieval from space: the Soil Moisture and Ocean Salinity (SMOS) mission. *IEEE Trans Geosci Remote Sens* 39:1729–1735
34. Prigent C, Aires F, Rossow WB (2006) Land surface microwave emissivities over the globe for a decade. *Bull Am Meteorol Soc* 87:1573–1584
35. Kerr YH (2007) Soil moisture from space: where are we? *Hydrogeol J* 15:117–120
36. Kerr YH, Waldteufel P, Wigneron JP, Delwart S, Cabot F, Boutin J, Escorihuela MJ, Font J, Reul N, Gruhier C, Juglea SE, Drinkwater MR, Hahne A, Martin-Neira M, Mecklenburg S (2010) The SMOS mission: new tool for monitoring key elements of the global water cycle. *Proc IEEE* 98:666–687
37. Font J, Camps AJ, Borges A, Martin-Neira M, Boutin J, Reul N, Kerr YH, Hahne A (2010) SMOS: the challenging sea surface salinity measurement from space. *Proc IEEE* 98:649–665
38. McMullan KD, Brown MA, Martin-Neira M, Rits W, Ekholm S, Marti J, Lemanczyk J (2008) SMOS: the payload. *IEEE Trans Geosci Remote Sens* 46:594–605
39. Merlin O, Walker JP, Chehbouni A, Kerr Y (2008) Towards deterministic downscaling of SMOS soil moisture using MODIS derived soil evaporation efficiency. *Remote Sens Environ* 112:3935–3946
40. Jackson TJ, Schmugge TJ (1991) Vegetation effects on the microwave emission of soils. *Remote Sens Environ* 36:203–212
41. Njoku EG, Entekhabi D (1996) Passive microwave remote sensing of soil moisture. *J Hydrol* 184:101–129
42. Aires F, Papa F, Prigent C (2013) A long-term, high-resolution wetland data set over the Amazon Basin, downscaled from a multi-wavelength retrieval using SAR data. *J Hydrometeorol* 14(2):594–607
43. Aires F, Papa F, Prigent C, Crétaux JF, Berge-Nguyen M (2013) Characterization and space/time downscaling of the inundation extent over the Inner Niger Delta using GIEMS and MODIS data. *J Hydrometeorol* 15(1):171–192. doi:[10.1175/JHM-D-13-032.1](https://doi.org/10.1175/JHM-D-13-032.1)
44. Entekhabi D, Njoku EG, O'Neill PE, Kellogg KH, Crow WT, Edelstein WN, Entin JK, Goodman SD, Jackson TJ, Johnson J, Kimball J, Piepmeier JR, Koster RD, Martin N, McDonald KC, Moghaddam M, Moran S, Reichle R, Shi JC, Spencer MW, Thurman SW, Tsang L, Van Ziel J (2010) The Soil Moisture Active Passive (SMAP) mission. *Proc IEEE* 98:704–716
45. Piles M, Entekhabi D, Camps A (2009) A change detection algorithm for retrieving high-resolution soil moisture from SMAP radar and radiometer observations. *IEEE Trans Geosci Remote Sens* 47:4125–4131
46. Anderson MP (2007) Introducing groundwater physics. *Phys Today* 60:42–47
47. Younger PL (2007) *Groundwater in the environment: an introduction*. Blackwell, Oxford, p 318
48. Hutti B, Nijagunappa R (2011) Application of geoinformatics in water resources management of semi-arid regions, North Karnataka, India. *Int J Geomatics Geosci* 2:373–382
49. Purkis S, Klemas V (2011) *Remote sensing and global environmental change*. Wiley-Blackwell, Oxford, p 367
50. Pool DR, Eychaner JH (1995) Measurements of aquifer storage change and specific yield using gravity surveys. *Ground Water* 33:425–432
51. Ramillien G, Frappart F, Cazenave A, Güntner A (2005) Time variations of the land water storage from an inversion of 2 years of GRACE geoids. *Earth Planet Sci Lett* 235:283–301
52. Swenson S, Wahr J, Milly PCD (2003) Estimated accuracies of regional water storage variations inferred from the Gravity Recovery and Climate Experiment (GRACE). *Water Resour Res* 39:12–23
53. Schmidt R, Schwinzer P, Flechtner F, Reigber C, Guntner A, Doll P, Ramillien P, Cazenave A, Petrovic S, Jochmann H, Wunsch J (2006) GRACE observations of changes in continental water storage. *Global Planet Change* 50:112–126

54. Rodell M, Famiglietti JS (2002) The potential for satellite-based monitoring of groundwater storage changes using GRACE: the High Plains aquifer, Central US. *J Hydrol* 263:245–256
55. Yirdaw SC, Snelgrove KR, Agboma CO (2008) GRACE satellite observations of terrestrial moisture changes for drought characterization in the Canadian Prairie. *J Hydrol* 356:84–92
56. Li B, Rodell M, Zaitchik BM, Reichle RH, Koster RD, Van Dam TM (2012) Assimilation of GRACE terrestrial water storage into a land surface model: evaluation and potential value for drought monitoring in western and central Europe. *J Hydrol* 446–447:103–115
57. Watkins MM (2004) Bowie lecture: time variable gravity measurements come of age. *Eos* 85 (47): Fall Meeting Supplement, Abstract G24A-01
58. Machiwal D, Jha MK, Mal BC (2011) Assessment of groundwater potential in a semi-arid region of India using remote sensing, GIS and MCDM techniques. *Water Resour Manag* 25:1359–1386
59. Gramling C (2013) Kenyan find heralds new era in water prospecting. *Science* 341:1327
60. Fetter CW (2001) Applied hydrogeology, 4th edn. Prentice-Hall, Upper Saddle River, p 598
61. Klemas V (2011) Remote sensing of sea surface salinity: an overview with case studies. *J Coastal Res* 27:830–838
62. Klemas V (2012) Remote sensing of coastal plumes and ocean fronts: overview and case study. *J Coastal Res* 28:1–7
63. Kolokoussis P, Karathanassi V, Rokos D, Argialas D, Karageorgis AP, Georgopoulos D (2011) Integrating thermal and hyperspectral remote sensing for the detection of coastal springs and submarine groundwater discharges. *Int J Remote Sens* 32:8231–8251
64. Loheide S (2009) A thermal remote sensing tool for mapping spring and diffuse groundwater discharge to streams. U.S. Geological survey report. <http://water.usgs.gov/wri/o8grants/2008WI192B.html>. Accessed 15 Oct 2014
65. Thomson KPB, Nielsen G (1980) Groundwater discharge detection along the coasts of the Arabian Gulf and the Gulf of Oman using thermal infrared imagery. In: Proceedings of the 14th international symposium on remote sensing of environment, San Jose, Costa Rica, 23–30 Apr 1980, pp 835–843
66. Klemas V (2013) Airborne remote sensing of coastal features and processes: an overview. *J Coastal Res* 29:239–255
67. Di Martino G, Tonielli R (2010) Freshwater runoff effects on shallow-water multibeam surveys: using multibeam data processing to characterize submarine freshwater springs. *Sea Technology*, May 2010, pp 10–13
68. Jensen JR (2007) Remote sensing of the environment: an earth resource perspective. Prentice-Hall, Englewood Cliffs, p 608
69. Klemas V (2013) Remote sensing of wetland biomass: an overview. *J Coastal Res* 29:1016–1028
70. Cihlar J, St. Laurent A, Dyer JA (1991) Relation between the normalized difference vegetation index and ecological variables. *Remote Sens Environ* 35:279–298
71. Goward SN, Markham B, Dye DG, Dulaney W, Yang J (1991) Normalized difference vegetation index measurements from the advanced very high resolution radiometer. *Remote Sens Environ* 35:257–277
72. Young SS, Wang CY (2001) Land-cover change analysis of China using global-scale Pathfinder AVHRR Landcover (PAL) data, 1982–92. *Int J Remote Sens* 22:1457–1477
73. Yuan D, Elvidge CD, Lunetta RS (1998) Survey of multispectral methods for land cover change analysis. In: Lunetta RS, Elvidge CD (eds) Remote sensing change detection: environmental monitoring methods and applications. Ann Arbor, Chelsea, pp 21–40
74. Dong J, Kaufmann RK, Myneni RB, Tucker CJ, Kauppi PE, Liski J, Buermann W, Alexeyev V, Hughes MK (2003) Remote sensing estimates of boreal and temperate forest woody biomass: carbon pools, sources, and sinks. *Remote Sens Environ* 84:393–410
75. Gower ST, Kucharik CJ, Norman JM (1999) Direct and indirect estimation of leaf area index, fAPAR and net primary production of terrestrial ecosystems. *Remote Sens Environ* 70:29–51

76. Ku NW, Popescu SC, Ansley RJ, Perotto-Baldivieso HL, Fillippi AN (2012) Assessment of available rangeland woody plant biomass with a terrestrial lidar system. *Photogramm Eng Remote Sens* 78:349–361
77. Peregon A, Maksyutov S, Kosykh NP, Mironycheva-Tokareva NP (2008) Map-based inventory of wetland biomass and net primary production in Western Siberia. *J Geophys Res* 113:1–12
78. Riegel B (2012) A comparison of remote sensing methods for estimating above-ground carbon biomass at a wetland restoration area in the southeastern coastal plain. <http://dukespace.lib.duke.edu/dspace/handle/10161/5164>. Accessed 15 Oct 2012
79. Running SW, Nemani RR, Heinsch FA, Zhao M, Reeves M, Hashimoto H (2004) A continuous satellite-derived measure of global terrestrial primary production. *Bioscience* 54:547–560
80. Lucas R, Armston J, Fairfax J, Fensham R, Dwyer J, Bowen M, Eyre T, Laidlaw M, Shimada M (2010) An evaluation of the ALOS PALSAR L-band backscatter- above ground biomass relationship over Queensland, Australia. *IEEE J Sel Top Earth Obs Remote Sens* 3:576–593
81. Graham S (2000) Drought: the creeping disaster. NASA Earth Observatory, August 28, 2000. <http://earthobservatory.nasa.gov/Features/DroughtFacts/>. Accessed 11 Apr 2014
82. Weier J, Herring D (2000) Measuring Vegetation (NDVI & EVI). NASA Earth Observatory, August 30, 2000. <http://earthobservatory.nasa.gov/Features/MeasuringVegetation/>. Accessed 11 Apr 2014
83. Hao Z, AghaKouchak A (2014) A nonparametric multivariate multi-index drought monitoring framework. *J Hydrometeorol* 15:89–101
84. Momtaz F, Nakhjiri N, AghaKouchak A (2014) Toward a drought cyber infrastructure system. *Eos* 95(22):182–183
85. Leibowitz SG (2003) Isolated wetlands and their functions: an ecological perspective. *Wetlands* 23:517–531
86. Semlitsch RD, Bodie JR (1998) Are small, isolated wetlands expendable? *Conserv Biol* 12:1129–1133
87. Winter TC, Labaugh JW (2003) Hydrologic considerations in defining isolated wetlands. *Wetlands* 23:532–540
88. Dahl TE (2006) Status and trends of wetlands in the conterminous United States 1998 to 2004. U.S. Department of the Interior, Fish and Wildlife Service, Washington, DC, p 112
89. Kelly M, Tuxen K (2009) Remote sensing support for tidal wetland vegetation research and management. In: Yang X (ed) *Remote sensing and geospatial technologies for coastal ecosystem assessment and management*. Springer, Berlin, pp 341–363
90. Ozesmi SL, Bauer ME (2002) Satellite remote sensing of wetlands. *Wetlands Ecol Manag* 10:381–402
91. Prigent C, Matthews E, Aires F, Rossow WB (2001) Remote sensing of global wetland dynamics with multiple satellite data sets. *Geophys Res Lett* 28:4631–4634
92. Tiner RW (1996) Wetlands. In: *Manual of photographic interpretation*, 2nd edn. American Society for Photogrammetry and Remote Sensing, Falls Church, Virginia, p 2440
93. Lunetta RS, Balogh ME (1999) Application of multi-temporal Landsat 5 TM imagery for wetland identification. *Photogramm Eng Remote Sens* 65:1303–1310
94. Baker C, Lawrence R, Montagne C, Patten D (2006) Mapping wetlands and riparian areas using Landsat ETM+ imagery and decision-based models. *Wetlands* 27:465–474
95. De Roeck ER, Verhoest NEC, Miya MH, Lievens H, Batelaan O, Thomas A, Brendonck L (2008) Remote sensing and wetland ecology: a South African case study. *Sensors* 8:3542–3556
96. Frohn RC, Reif M, Lane C, Autrey B (2009) Satellite remote sensing of isolated wetlands using object-oriented classification of Landsat-7 data. *Wetlands* 29:931–941
97. Tiner RW (2003) Geographically isolated wetlands of the United States. *Wetlands* 23:494–516

98. Klemas V (2013) Remote sensing of emergent and submerged wetlands: an overview. *Int J Remote Sens* 34:6286–6320
99. Wulder MA, Hall RJ, Coops NC, Franklin SE (2004) High spatial resolution remotely sensed data for ecosystem characterization. *Bioscience* 54:511–521
100. McCoy R (2005) Field methods in remote sensing. Guilford, New York, p 161
101. Ellis JM, Dodd HS (2000) Applications and lessons learned with airborne multispectral imaging. In: Fourteenth international conference on applied geological remote sensing, Las Vegas, Nevada, 6–8 Nov 2000
102. Lyon JG, McCarthy J (1995) Wetland and environmental applications of GIS. Lewis, New York, p 400
103. Hays RL (2009) Vegetation patterns and nutrient cycling in Delaware Bay salt marshes, Great Marsh (Lewes) and Webbs Marsh (South Bowers), Delaware. PhD Dissertation, University of Delaware, Lewes, p 384
104. Jensen RR, Mausel P, Dias N, Gonser R, Yang C, Everitt J, Fletcher R (2007) Spectral analysis of coastal vegetation and land cover using AISA+ hyperspectral data. *Geocarto Int* 22:17–28
105. Schmid T, Koch M, Gumuzzio J (2005) Multisensor approach to determine changes of wetland characteristics in semiarid environments in central Spain. *IEEE Trans Geosci Remote Sens* 43:2516–2525
106. Schmidt KS, Skidmore AK, Kloosterman EH, Van Oosten H, Kumar L, Janssen JAM (2004) Mapping coastal vegetation using an expert system and hyperspectral imagery. *Photogramm Eng Remote Sens* 70:703–716
107. Yang C, Everitt JH, Fletcher RS, Jensen JR, Mausel PW (2009) Mapping black mangrove along the south Texas gulf coast using AISA+ hyperspectral imagery. *Photogramm Eng Remote Sens* 75:425–436
108. Yang J, Artigas FJ (2009) Mapping salt marsh vegetation by integrating hyperspectral and LiDAR remote sensing. In: Wang J (ed) Remote sensing of coastal environments. CRC, Boca Raton, pp 173–187
109. Gilmore MS, Civco DL, Wilson EH, Barrett N, Prisloe S, Hurd JD, Chadwick C (2009) Remote sensing and in situ measurements for delineation and assessment of coastal marshes and their constituent species. In: Wang J (ed) Remote sensing of coastal environments. CRC, Boca Raton, pp 261–280
110. Adam E, Mutanga O, Rugege D (2010) Multispectral and hyperspectral remote sensing for identification and mapping of wetland vegetation: a review. *Wetlands Ecol Manag* 18:281–296
111. Simard M, Fatoyinbo LE, Pinto N (2009) Mangrove canopy 3D structure and ecosystem productivity using active remote sensing. In: Wang J (ed) Remote sensing of coastal environments. CRC, Boca Raton, pp 61–78
112. Wang Y (2009) Remote sensing of coastal environments: an overview. In: Wang J (ed) Remote sensing of coastal environments. CRC, Boca Raton, pp 1–24
113. Baghdadi N, Bernier M, Gauthier R, Neeson I (2001) Evaluation of C-band SAR data for wetlands mapping. *Int J Remote Sens* 22:71–88
114. Lang MW, McCarty GW (2008) Remote sensing data for regional wetland mapping in the United States: trends and future prospects. In: Russo RE (ed) Wetlands: ecology, conservation and restoration. Nova Science, Hauppauge, pp 73–112
115. Novo EMLM, Costa MPF, Mantovani JE, Lima IBT (2002) Relationship between macrophyte stand variables and radar backscatter at L and C band, Tucuruí reservoir, Brasil. *Int J Remote Sens* 23:1241–1260
116. Rosenqvist A, Finlayson CM, Lowry J, Taylor D (2007) The potential of long-wavelength satellite-borne radar to support implementation of the Ramsar Wetland Convention. *Aquat Conserv Mar Freshw Ecosyst* 17:229–244
117. Townsend PA (2000) A quantitative fuzzy approach to assess mapped vegetation classifications for ecological applications. *Remote Sens Environ* 72:253–267

118. Townsend PA (2002) Relationships between forest structure and the detection of flood inundation in forested wetlands using C-band SAR. *Int J Remote Sens* 23:443–460
119. Hall DK (1996) Remote sensing applications to hydrology: imaging radar. *Hydrol Sci J* 41:609–624
120. Kasischke E, Melack J, Dobson M (1997) The use of imaging radars for ecological applications: a review. *Remote Sens Environ* 59:141–156
121. Kasischke E, Bourgeau-Chavez L (1997) Monitoring South Florida wetlands using ERS-1 SAR imagery. *Photogramm Eng Remote Sens* 63:281–291
122. Lang MW, Kasischke ES (2008) Using C-band synthetic aperture radar data to monitor forested wetland hydrology in Maryland's Coastal Plain, USA. *IEEE Trans Geosci Remote Sens* 46:535–546
123. Phinn SR, Stow DA, Van Mouwerik D (1999) Remotely sensed estimates of vegetation structural characteristics in restored wetlands, Southern California. *Photogramm Eng Remote Sens* 65:485–493
124. Rao BRM, Dwivedi RS, Kushwaha SPS, Bhattacharya SN, Anand JB, Dasgupta S (1999) Monitoring the spatial extent of coastal wetlands using ERS-1 SAR data. *Int J Remote Sens* 20:2509–2517
125. Wilson BA, Rashid H (2005) Monitoring the 1997 flood in the Red River Valley using hydrologic regimes and RADARSAT imagery. *Can Geogr* 49:100–109
126. Toyra JA, Pietroniro A, Martz W, Prowse TD (2002) A multi-sensor approach to wetland flood monitoring. *Hydrol Process* 16:1569–1581
127. Costa MPF, Telmer KH (2007) Mapping and monitoring lakes in the Brazilian Pantanal wetland using synthetic aperture radar imagery. *Aquat Conserv Mar Freshw Ecosyst* 17:277–288
128. Dwivedi R, Rao B, Bhattacharya S (1999) Mapping wetlands of the Sundarban delta and its environs using ERS-1 SAR data. *Int J Remote Sens* 20:2235–2247
129. Kasischke ES, Smith KB, Bourgeau-Chavez LL, Romanowicz EA, Brunzell S, Richardson CJ (2003) Effects of seasonal hydrologic patterns in south Florida wetlands on radar backscatter measured from ERS-2 SAR imagery. *Remote Sens Environ* 88:423–441
130. Harris J, Digby-Argus S (1986) The detection of wetlands on Radar imagery. In: *Proceedings of the tenth Canadian symposium on remote sensing*, Edmonton, Alberta, May 1986
131. Wdowinski S, Hong SH (2014) Wetland InSAR. In: Tiner R, Klemas V, Lang M (eds) *Advances in wetland mapping*. CRC, Boca Raton
132. Wdowinski S, Amelung F, Miralles-Wilhelm F, Dixon TH, Carande R (2004) Space-based measurements of sheet-flow characteristics in the Everglades wetland, Florida. *Geophys Res Lett* 31:L15503
133. Wdowinski S, Kim SW, Amelung F, Dixon TH, Miralles-Wilhelm F, Sonenshein R (2008) Space-based detection of wetlands' surface water level changes from L-band SAR interferometry. *Remote Sens Environ* 112:681–696
134. Deng M, Di L, Han W, Yagci AL, Peng C, Heo G (2013) Web-service-based monitoring and analysis of global agricultural drought. *Photogramm Eng Remote Sens* 79:926–943
135. Mu Q, Zhao M, Kimball JS, McDowell MG, Running S (2013) A remotely sensed global terrestrial drought index. *Bull Am Meteorol Soc* 94:83–98
136. Narasimhan B, Srinivasan R (2005) Development and evaluation of soil moisture deficit index (SMDI) and evapotranspiration deficit index (ETDI) for agricultural drought monitoring. *Agr Forest Meteorol* 133:69–88
137. Dutta D, Kundu A, Patel NR (2013) Predicting agricultural drought in eastern Rajasthan of India using NDVI and standardized precipitation index. *Geocarto Int* 28:192–209
138. NOAA/CPC (2014) Drought: the creeping disaster. NASA earth observatory feature article, http://earthobservatory.nasa.gov/Features/DroughtFacts/drought_facts_4.php. Accessed 28 July 2014

Advances in Watershed Science and Assessment

Younos, T.; Parece, T.E. (Eds.)

2015, XX, 292 p. 98 illus., 77 illus. in color., Hardcover

ISBN: 978-3-319-14211-1